Characterization of the Calcium-sensitive Voltage-gated Delayed Rectifier Potassium Channel in Isolated Guinea Pig Hepatocytes

SHIN-ICHI KOUMI, RYOICHI SATO*, TATSUYUKI HORIKAWA, TAKUMI ARAMAKI, AND HIDEMASA OKUMURA

From the First Department of Internal Medicine, Nippon Medical School, Tokyo 113, and *First Department of Internal Medicine, Kinki University School of Medicine, Osaka 589, Japan

ABSTRACT The voltage-dependent K^+ channel was examined in enzymatically isolated guinea pig hepatocytes using whole-cell, excised outside-out and inside-out configurations of the patch-clamp technique. The resting membrane potential in isolated hepatocytes was -25.3 ± 4.9 mV ($n = 40$). Under the whole-cell voltage-clamp, the time-dependent delayed rectifier outward current was observed at membrane potentials positive to -20 mV at physiological temperature (37°C). The reversal potential of the current, as determined from tail current measurements, shifted by ~ 57 mV per 10-fold change in the external K^+ concentration. In addition, the current did not appear when K^+ was replaced with Cs^+ in the internal and external solutions, indicating that the current was carried by K^+ ions. The envelope test of the tails demonstrated that the growth of the tail current followed that of the current activation. The ratio between the activated current and the tail amplitude was constant during the depolarizing step. The time course of growth and deactivation of the tail current were best described by a double exponential function. The current was suppressed in Ca^{2+}-free, 5 mM EGTA internal or external solution (pCa > 9). The activation curve (P_∞ curve) was not shifted by changing the internal Ca^{2+} concentration ($[Ca^{2+}]_i$). The current was inhibited by bath application of 4-aminopyridine or apamin. α_1-Adrenergic stimulation with noradrenaline enhanced the current but β-adrenergic stimulation with isoproterenol had no effect on the current. In single-channel recordings from outside-out patches, unitary current activity was observed by depolarizing voltage-clamp steps whose slope conductance was 9.5 ± 2.2 pS ($n = 10$). The open time distribution was best described by a single exponential function with the mean open lifetime of 18.5 ± 2.6 ms ($n = 14$), while at least two exponentials were required to fit the closed time distributions with a time constant for the fast component of 2.0 ± 0.3 ms ($n = 14$) and that for the slow component of 47.7 ± 5.9 ms ($n = 14$). Ensemble averaged current exhibited

Address correspondence to Shin-ichi Koumi, at his present address, Department of Medicine, Reingold ECG Center, Northwestern University Medical School, 303 East Chicago Avenue, Chicago, IL, 60611-3008.

J. GEN. PHYSIOL. © The Rockefeller University Press · 0022-1295/94/07/0147/25 $2.00
Volume 104 July 1994 147–171

delayed rectifier nature which was consistent with whole-cell measurements. In excised inside-out patch recordings, channel open probability was sensitive to $[Ca^{2+}]_i$. The concentration of Ca^{2+} at the half-maximal activation was 0.031 μM. These results suggest that guinea pig hepatocytes possess voltage-gated delayed rectifier K^+ channels which are modified by intracellular Ca^{2+}.

INTRODUCTION

Membrane potential is directly related to the physiological functions in the liver. Some hormonal agents including insulin (Moore, 1983), glucagon (Graf and Petersen, 1978), or α-adrenergic stimulators (Haylett and Jenkinson, 1972*a,b;* DeWitt and Putney, 1984) have been shown to regulate the K^+ transport through the liver cell membrane. The mechanisms of ion transport across the liver cell membrane have been studied in a variety of preparations from different species by measuring intracellular ion concentrations and net isotope fluxes. The hormonal stimulation-induced increase of K^+ permeability was demonstrated using intracellular recording and measurements of ^{42}K flux in guinea pig liver slices (Haylett and Jenkinson, 1972*a,b;* Haylett, 1976). DeWitt and Putney (1984) used ^{86}Rb or $^{42}K^+$ to monitor K^+ movements in guinea pig hepatocytes. Electrophysiological methods have been used to identify voltage-dependent K^+ channels in various nonexcitable cells (Van Driessche and Zeiske, 1985). Recently, the patch-clamp technique has been applied to examine membrane ion conductances in isolated rat hepatocytes (Bear and Petersen, 1987; Henderson, Graf, and Boyer, 1989). Bear and Petersen (1987) demonstrated Ca^{2+}-activated K^+ channels ($I_{K(Ca)}$) evoked by L-alanine, while Henderson et al. (1989) reported inwardly-rectifying K^+ channels. A delayed rectifier type of K^+ channel current has been described in avian hepatocytes and the current was Ca^{2+} insensitive (Marchetti, Premont, and Brown, 1988). The properties of membrane ion conductances in guinea pig hepatocytes have also been evaluated in some detail, including whole-cell K^+ currents (Capiod and Ogden, 1989*a*) as well as single channel $I_{K(Ca)}$ (Capiod and Ogden, 1989*b*). These studies in guinea pig hepatocytes showed that the current exhibited ohmic conductance in the current-voltage (*I-V*) relationship.

In contrast, the voltage-gated channel has not been defined in guinea pig hepatocytes. The voltage dependence and Ca^{2+} sensitivity of the channel is also still undetermined. The purpose of this study was to assess the underlying nature of voltage and Ca^{2+} sensitivity of membrane ionic channels in isolated guinea pig hepatocytes.

Some of these results have been reported in preliminary form (Koumi, Sato, Kushikata, Muramatsu, Horikawa, Aramaki, and Okumura, 1990; Koumi, Sato, Nagano, Horikawa, Aramaki, and Okumura, 1991).

MATERIALS AND METHODS

Cell Preparation

Single guinea pig hepatocytes were enzymatically dissociated according to the method described previously (Graf, Gautam, and Boyer, 1984; Gautam, Ng, and Boyer, 1987). Briefly, adult guinea pigs (Hartley) of either sex, weighing 300–400 g were anesthetized with pentobarbitone (60 mg/kg, i.p.), and the portal vein was cannulated. Liver perfusion was

initiated with a Ca^{2+}-free solution (first perfusion solution) for 10 min at a flow rate of 5 ml/min. The perfusate was switched to a solution containing 4 mM Ca^{2+} and 0.5 mg/ml of collagenase (type I, Sigma Chemical Co., St. Louis, MO) for 10 min at 10 ml/min (second perfusion solution). The solutions were gassed with 100% O_2 and warmed to 37°C. After these perfusions, the liver was excised and then minced in Hank's balanced salt solution (BSS). The cells were filtered through a 150-μm nylon mesh, and washed three times by centrifugation at 100 *g* for 3 min. The cell pellets were resuspended in Hank's BSS and used within 6 h after the isolation.

Isolated cell viability was assessed by the trypan blue exclusion technique after completion of the isolation procedure. The preparation was discarded if <80% of the cells excluded trypan blue. The dissociation procedure yielded spherical, smooth cells with a diameter of 19.7 ± 3.1 μm (n = 46).

Solutions and Chemicals

The first solution perfused via the portal vein cannulation contained (in millimolar): NaCl 140, KCl 5.4, NaH_2PO_4 0.6, Na_2HPO_4 0.4, EGTA (ethylene glycol-bis-(β-aminoethylether) *N,N,N′,N′*-tetraacetate) 0.5, $NaHCO_3$ 4.2, glucose 5, and *N′*-2-hydroxyethylpiperazine-*N′*-2-ethanesulfonic acid (HEPES)-NaOH buffer 9.6, brought to pH 7.2 with NaOH. The second perfusion solution contained (in millimolar): NaCl 140, KCl 5.4, $CaCl_2$ 4.0, NaH_2PO_4 0.6, Na_2HPO_4 0.4, $NaHCO_3$ 4.2, HEPES-NaOH buffer 9.6, and collagenase 0.5 (pH = 7.5). Hank's balanced salt solution (BSS) contained (in millimolar): NaCl 140, KCl 5.4, $CaCl_2$ 1.3, $MgCl_2$ 1.0, $MgSO_4$ 1.7, NaH_2PO_4 0.6, Na_2HPO_4 0.4, $NaHCO_3$ 4.2, glucose 5 (pH = 7.2). The external normal Tyrode's solution used during whole-cell or excised outside-out patch recordings contained (in millimolar): NaCl 142, KCl 5.4, $CaCl_2$ 1.8, $MgCl_2$ 0.5, glucose 10, HEPES 8 (pH = 7.3). Ca^{2+}-free external solution contained (in millimolar): NaCl 142, KCl 5.4, $MgCl_2$ 0.5, glucose 10, HEPES 8, EGTA 5 (pH = 7.3). Ca^{2+}-free high Mg^{2+} solution contained (in millimolar): NaCl 142, KCl 5.4, $MgCl_2$ 2.3, glucose 10, HEPES 8, EGTA 5 (pH = 7.3). Pipette solution (standard internal solution) used during whole-cell or excised outside-out patch recordings contained (in millimolar): KCl 150, $MgCl_2$ 1.0, EGTA 5; HEPES 8 (pH = 7.3 with KOH). Free Ca^{2+} concentration ($[Ca^{2+}]$) was adjusted to 0.1 μM (pCa = 7) by adding $CaCl_2$. Ca^{2+}-unbuffered internal solution was (in millimolar): KCl 150, $MgCl_2$ 1.0, HEPES 8 (pH = 7.3). Cl^--free external solution contained (in millimolar): Na gluconate 142, K gluconate 5.4, $CaSO_4$ 1.8, $MgSO_4$ 0.5, glucose 10, HEPES 8 (pH = 7.3). Cl^--free internal solution contained (in millimolar): K gluconate 150, $MgSO_4$ 1.0, HEPES 8 (pH = 7.3). In excised inside-out patch recordings, normal Tyrode's solution was used for the pipette solution and bath solution (cytosolic side) contained (in millimolar): KCl 150, $CaCl_2$ 0.5, $MgCl_2$ 1.0, HEPES 8 (pH = 7.3). The free Ca^{2+} in each solution was adjusted by adding EGTA to obtain activities ranging from $<10^{-9}$ M to 1.0×10^{-3} M (Fabiato and Fabiato, 1979).

The recording chamber (0.18 ml) was continuously perfused with bath solution at the perfusion rate of 5 ml/min. Temperature of the bath was monitored and was maintained at 37 ± 1°C using a Peltier thermo-electrical device. Several experiments were carried out at room temperature (20–21°C) without using a Peltier device.

4-aminopyridine (4-AP), apamin, noradrenaline, isoproterenol, forskolin, glucagon, and insulin were applied to the external solution, while adenosine-3′,5′-cyclic monophosphate (cAMP) was included in the pipette solution in some whole-cell experiments. All chemicals were purchased from Sigma Chemical Co.

Electrical Recordings

Membrane currents were recorded using the patch-clamp technique (Hamill, Marty, Neher, Sakmann, and Sigworth, 1981) and an Axopatch-1C amplifier (Axon Instruments, Inc., Foster

City, CA). The pipettes were pulled in two stages from hard glass tubing (Narishige Scientific Instruments Laboratories, Tokyo) using a vertical microelectrode puller (Type PE-2, Narishige Scientific Instruments Laboratories) and then fire polished using a microforge (Model MF-83, Narishige Scientific Instruments Laboratories). Electrodes had a resistances of 2–3 MΩ for whole-cell recording and 6–8 MΩ for single channel recording when filled with appropriate standard internal solutions. Inverted voltage-clamp pulses were applied to the bath through an Ag-AgCl pellet-KCl agar bridge with the pipette potential maintained at ground level. The head stage of the voltage-clamp circuit was set up with an ultra-low bias current operational amplifier. The feedback resistance of the head stage was 500 MΩ for recording whole-cell current and 50 GΩ for recording single-channel current. The output of the voltage-clamp amplifier was adjusted to give zero current when the tip of the pipette (filled with internal solution) was immersed in the bath containing control external solution.

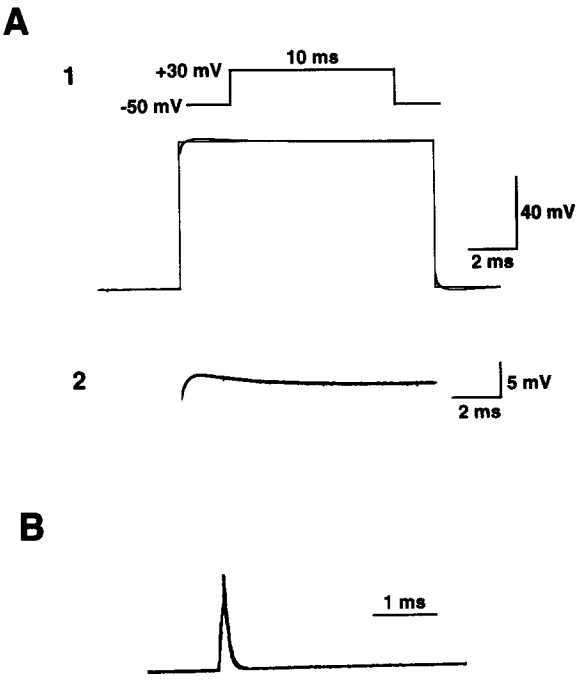

FIGURE 1. Adequacy of voltage control evaluated by an independent microelectrode in an isolated guinea pig hepatocyte. (*A*) After the whole-cell configuration was achieved, the cell was impaled with an independent high resistance microelectrode (40 MΩ with 3 M KCl) at another part of the cell. Voltage-clamp pulse protocol is shown in inset of *A1*. Initially, the membrane was voltage-clamped at −50 mV by the patch-electrode and then the voltage-clamp test pulse to +30 mV for 10 ms was applied. *A1* shows the superimposed trace of the square voltage command applied from the patch electrode and the actual transmembrane voltage recorded from the independent microelectrode. The depolarizing step section of *A1* is shown with more detail on an expanded voltage base in *A2*. The maximal deviation of the actual transmembrane voltage from the voltage command was 1.6 mV in this cell. Current and time calibration are shown in the lower right corner. (*B*) Shows an example of the capacitative transient obtained using a 10-mV depolarizing pulse before employing series resistance compensation. The decay phase was well fitted by a single exponential function with a time constant of 160.7 μs in this cell.

For whole-cell recording, the adequacy of the voltage control had been tested by preliminary experiments monitoring the membrane potential using an independent microelectrode (Fig. 1 *A*). A guinea pig hepatocyte was attached to a patch pipette and once the whole-cell configuration was achieved, the cell was impaled with an independent high resistance microelectrode (40–45 MΩ with 3 M KCl) at another part of the cell. Initially, the membrane was voltage-clamped at −50 mV by the patch-electrode and then the voltage-clamp test pulse

to +30 mV for 10 ms was applied. Fig. 1, *A1* shows the superimposed trace of the square voltage command applied from the patch electrode and the actual transmembrane voltage recorded from the independent microelectrode. Fig. 1, *A2* shows the actual transmembrane voltage during the depolarizing step on an expanded voltage base. The averaged maximal deviation of the transmembrane voltage from the command voltage was 1.5 ± 0.3 mV (n = 21). Sufficient voltage control was achieved within ~2–3 ms in all of the cells tested. Fig. 1 *B* shows an example of the capacitative transient obtained using a 10-mV depolarizing pulse. The decay phase was well fit by a single exponential function with a mean time constant of the capacitative transient was 151.0 ± 24.1 μs (n = 44). Values of cell capacitance (C_m) were estimated from capacitative transients using equation: $C_m = Q/\Delta V$, where ΔV is the amplitude of voltage step and Q is the total charge displayed during the voltage step. Q was estimated by integration of the capacitative transient. The mean value of the cell capacitance was 31.4 ± 5.2 pF (n = 44). The value was consistent with studies made by Capiod and Ogden (1989*a*), who estimated the cell capacitance of 30.6 pF in guinea pig hepatocytes. The mean series resistance (R_s) was 4.8 ± 1.0 MΩ (n = 44). Compensation for this series resistance was performed empirically by applying electronic series resistance compensation to a maximum level of 70–80% before producing current oscillations. The series resistance arising mainly at the electrode tip was compensated for by summing a fraction of the converted current signal to the command potential and feeding it to the positive input of the operational amplifier. The leak current was linear in the voltage range −50 to +50 mV and was digitally subtracted in this voltage range based on the line extrapolated through the current values more negative than +20 mV. After gaining access in the whole-cell patch-clamp configuration, hepatocytes were allowed to "stabilize" electrophysiologically for 5–15 min before collecting data. Resting membrane potential was measured by the whole-cell current-clamp mode.

Single channel currents were monitored with a storage oscilloscope (Type 5113, Tektronix, Inc., Beaverton, OR) and were stored continuously on digital audio tape (R-60DM, MAXELL, Tokyo) using a PCM data recording system (RD-100T, TEAC, Tokyo). The single channel events were reproduced and filtered off-line with a cut-off frequency of 2 KHz through an eight-pole low-pass Bessel filter (48 dB/octave, model 902-LPF, Frequency Devices, Inc., Haverhill, MA), digitized with 14-bit resolution at a sample rate of 10 KHz. Leakage currents during voltage step recording were canceled by subtracting each trace from the average current traces without events. The data were analyzed on a computer (PC-9801, NEC, Tokyo) using locally written analysis programs that are based on the half-amplitude threshold analysis method of Colquhoun and Sigworth (1983). Channel transitions were calculated using an averaging technique for determining channel amplitude. The measurements derived from the channel transitions were collected into histograms to allow an analysis of the single-channel kinetics. Mean dwell times were determined from the sum of exponential fits to the distributions of open and closed times recorded from patches with only one channel.

Mathematical Analysis

The time course of the activation and deactivation of the tail current can be fit by the nonlinear regression method to the following equation:

$$I(t) = I_f \exp(-t/\tau_f) + I_s \exp(-t/\tau_s) + I_\infty \quad (1)$$

where I_f and τ_f represent the amplitude and the time constant for the fast component, I_s and τ_s represent those for the slow component, I_∞ denotes the steady state current.

The fitted curve for steady state activation (P_∞) was obtained using a Boltzmann's distribution:

$$P_\infty = 1/\{1 + \exp(E - V_h)/K\} \quad (2)$$

where V_h is the half-activation voltage and K is the slope factor.

The concentration-response curve was fitted by the least-squares method to the Hill equation:

$$y = P_{max}/\{1 + (IC_{50}/[M])^H\} \quad (3)$$

where P_{max} is the maximal effect, IC_{50} is the concentration at the half-maximal effect and H is the Hill coefficient.

Statistical Analysis

All curve fitting was performed with a non-linear least-square algorithm on a computer (PC-9801, NEC) using custom software. The results are expressed as mean ± SD. Differences between sample means were determined using *t* test or one-way analysis of variance. A *P* value <0.05 was considered statistically significant.

RESULTS

Whole-Cell Membrane Currents

The resting membrane potential measured by the whole-cell current-clamp mode in these cells was -25.3 ± 4.9 mV ($n = 40$). The value was consistent with studies made by Capiod and Ogden (1989*a*), who estimated the resting membrane potential of -27 mV.

Fig. 2 shows an example of a whole-cell membrane current family recorded from an isolated guinea pig hepatocyte after subtraction of linear leakage conductance at physiological temperature (37°C). Depolarizing voltage-clamp test pulses were applied for 2 s from a holding potential of -50 mV. The standard internal solution ($[Ca^{2+}] = 0.1$ μM) was used in the pipette solution and the external solution was the normal Tyrode's. The previously reported $I_{K(Ca)}$ is inactive at this level of internal Ca^{2+} concentration ($[Ca^{2+}]_i$) (Capiod and Ogden, 1989*b*). Whole-cell depolarizing voltage steps positive to -20 mV produced the time-dependent delayed rectifier outward current. Fig. 2 *B* shows the current-voltage (*I-V*) relationship. This current was found in 108 out of 136 cells (79.4%). The current was stable without rundown. In contrast, when the membrane current was measured at room temperature (20–21°C), the outward current was observed in 6 of 47 cells (12.8%). In addition, the current magnitude was smaller than that recorded at 37°C at all voltages and delayed rectifier property was weak in all six cells. The current magnitude was 0.12 ± 0.02 nA ($n = 6$) at 0 mV. The value was significantly smaller than that recorded at physiological temperature of 0.31 ± 0.03 nA ($n = 20$) at 0 mV ($P < 0.001$).

The ionic selectivity of this outward current was estimated by measuring tail currents using a double pulse protocol (Fig. 3). The cell was held at -50 mV and was depolarized to $+80$ mV for 2 s. This was followed by the clamp back pulse in the range of -10 to -100 mV. Fig. 3 *A* shows an example of the obtained tail currents. The averaged reversal potential of the tail current was -79.2 ± 4.2 mV ($n = 11$), which is close to the theoretical Nernst potential for a K^+ selective channel in the normal Tyrode's solution with external K^+ concentration ($[K^+]_o$) of 5.4 mM at 37°C (internal K^+ concentration $[K^+]_i = 150$ mM). The reversal potential was shifted to -41.0 ± 3.3 mV ($n = 11$) and -10.5 ± 2.1 mV ($n = 11$) when $[K^+]_o$ was increased to 20 and 100 mM, respectively. The regression line in semilogarithmic scale had a slope of 57 mV per 10-fold increase in $[K^+]_o$ (Fig. 3 *B*).

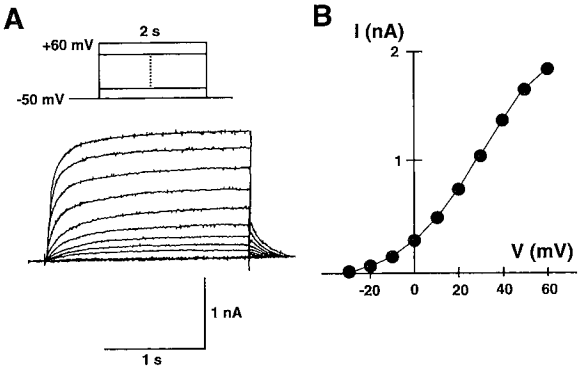

FIGURE 2. Whole-cell membrane currents in isolated guinea-pig hepatocytes. (*A*) Representative family of whole-cell outward currents recorded in normal Tyrode's solution at 37°C. The pipette solution was the standard internal ($[Ca^{2+}]$ = 0.1 μM). The voltage-clamp pulse protocol used to obtain the recordings is depicted in the inset; 2-s duration pulses to test potentials ranging from −40 to +60 mV in 10-mV increments were applied from a holding potential of −50 mV. The current was activated at potential positive to −20 mV and exhibited time-dependent increase (delayed rectification). Current and time calibration are shown in the lower right corner. (*B*) The current-voltage (*I-V*) relationship derived from the data in *A*. Each point (*circles*) was measured at the end point of the test pulse (2 s).

When K^+ was replaced with Cs^+ in the pipette solution, the delayed rectifier outward current did not appear (n = 8, data not shown). To test the effect of Cl^- on this outward current, the current was measured in the Cl^--free internal and external solutions. The current was unchanged in this condition (n = 5), suggesting that the current is not affected by Cl^-. These results indicate that this outward current is carried mainly by K^+ ions.

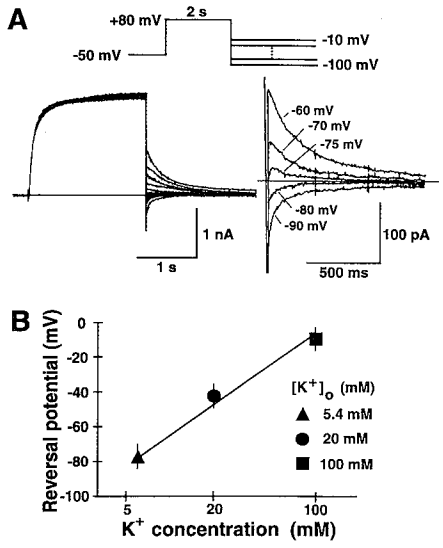

FIGURE 3. Reversal potential measurements for the delayed rectifier outward current. (*A*) Recordings of the tail current reversal potential which was determined using a double-pulse protocol in 5.4 mM external K^+. The pipette solution was the standard internal ($[K^+]$ = 150 mM, $[Ca^{2+}]$ = 0.1 μM). The voltage-clamp pulse protocol used to obtain the recordings is depicted in the inset; a 2-s depolarizing test pulse was applied to +80 mV from a holding potential of −50 mV, which was followed by the test pulse ranging from −10 to −100 mV. In this cell, the tail current inverted between −75 and −80 mV. The value is close to the calculated reversal potential. (*B*) The reversal potentials of the tail current were plotted semilogarithmically as a function of the extracellular K^+ concentrations ($[K^+]_o$). $[K^+]_o$ was changed to 5.4, 20, and 100 mM. Reversal potentials were −79.2 ± 4.2 mV at 5.4 mM (*triangle*), −41.0 ± 3.3 mV (*circle*) at 20 mM and −10.5 ± 2.1 mV (*square*) at 100 mM $[K^+]_o$. The vertical bar through each point represents the SD (n = 11 for each).

Time- and Voltage-dependent Kinetics of the Outward Current

To study the kinetic property of the delayed rectifier outward current, the envelope test (Noble and Tsien, 1969) was employed (Fig. 4). The depolarizing voltage steps were applied from a holding potential of −50 mV to +80 mV for durations ranging from 50 ms to 2 s which was followed by the repolarizing steps to −50 mV. The envelope of the tail currents parallels the growth of outward current during depolarization (Fig. 4 *A*). Relationship between magnitude of the activated outward current and that of the tail current was evaluated by measuring the ratio of the currents as a function of time during the depolarizing pulse (Fig. 4 *B*). The ratio averaged from four different cells was virtually unchanged during the depolarizing step (not significant statistically) and the averaged ratio was 2.35 ± 0.18 (n = 4).

The time course of the current activation was evaluated by measuring the time course of the growth of the tail current. The depolarizing voltage steps were applied

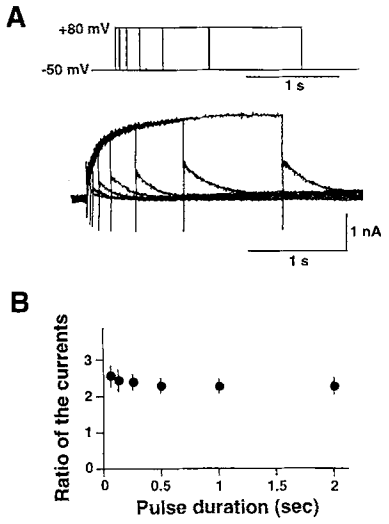

FIGURE 4. Envelope of tails test for the delayed rectifier outward current recorded using the standard internal and normal Tyrode's solution at 37°C. (*A*) A superimposed tracings of the tail currents onto the activating current. The voltage-clamp pulse protocol used to obtain the recordings is depicted in the inset; various durations (50 ms to 2 s) of test pulses to +80 mV were applied from a holding potential of −50 mV. The envelope of the tail currents parallels the growth of the outward current during depolarization. (*B*) The ratio of the currents (the outward current activated at +50 mV divided by the tail current) was plotted as a function of time during the depolarizing pulse. Each value was averaged from four different cells and was expressed as mean ± SD. The ratio was constant throughout the depolarizing pulse (not significant statistically).

from a holding potential of −50 mV to the test potentials ranging from +10 to +50 mV for durations ranging from 50 ms to 2 s which was followed by the repolarizing steps to −50 mV. The time course of the growth of the tail current was best described by a double exponential function at all test voltages and can be fit by the nonlinear regression method to Eq. 1. Fig. 5 *A* shows the plot of the averaged time constants (τ_f, τ_s) as a function of test voltages. The time constants exhibited bell-shaped-like voltage-dependence. The maximal values were given at +40 mV.

The time course of the current deactivation was evaluated by measuring the time course of the deactivation of the tail current. The voltage steps were applied from a holding potential of −50 mV to the conditioning potentials of +50 mV for 2 s which was followed by the repolarizing test potentials ranging from −50 to −10 mV. The

time course of deactivation of the tail current was determined by the exponential fitting of the decay phase of the tail current. The time course of deactivation of the tail current was also best described by a double exponential function at all test voltages and can be fit to Eq. 1. Fig. 5 *B* shows the plot of the averaged time constants (τ_f, τ_s) as a function of test voltages. The time constants became smaller with more negative test voltages.

Ca^{2+} Sensitivity of the Current

In guinea pig hepatocytes, intracellular Ca^{2+} appears to be a significant modulator of membrane conductances (Burgess, Claret, and Jenkinson, 1979; Cook and Haylett, 1985; Field and Jenkinson, 1987; Capiod, Field, Ogden and Sandford, 1987; Capiod and Ogden, 1989*a,b;* Ogden, Capiod, Walker, and Trentham, 1990).

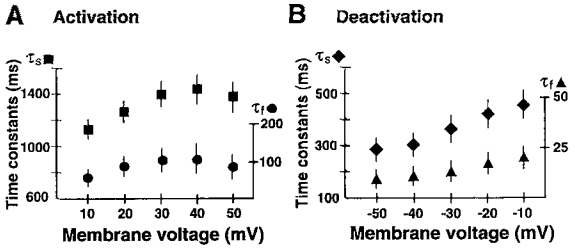

FIGURE 5. (*A*) Voltage-dependence of time course of the delayed rectifier outward current activation. The averaged time constants of the growth of the tail current (the fast component, τ_f, *circles;* and the slow component, τ_s, *squares*) were plotted as a function of voltage. The time course was evaluated by the tail current evoked by the clamp back step from the voltage-clamp pulses to various voltages between +10 and +50 mV from a holding potential of −50 mV. The vertical bar through each point represents the SD (n = 8 for each). (*B*) Voltage-dependence of time course of the delayed rectifier outward current deactivation. The averaged time constants of decay of the tail current (the fast component, τ_f, triangles; and the slow component, τ_s, *diamonds*) were plotted as a function of voltage. The time course was evaluated by the tail current evoked by the clamp back steps ranging from −50 to −10 mV from the conditioning depolarizing pulses to +50 mV for 2 s from a holding potential of −50 mV. The vertical bar through each point represents the SD (n = 6 for each).

The sensitivity of the delayed rectifier outward current on Ca^{2+} was examined by altering the concentration of Ca^{2+} in the external and internal solutions (Fig. 6). Effects of Ca^{2+}-free external solution on the current was first examined by switching the external solution from the normal Tyrode's ([Ca^{2+}] = 1.8 mM) to the Ca^{2+}-free solution containing 5 mM EGTA (pCa > 9). External Ca^{2+} can affect the level of cytosolic Ca^{2+} and Ca^{2+} influx is completely suppressed in Ca^{2+}-free external solution (Mauger, Poggioli, Guesdon, and Claret, 1984). For this experiment, the Ca^{2+}-unbuffered internal solution was used for the pipette solution. After 5–10 min exposure to the Ca^{2+}-free solution, the current amplitude was decreased (Fig. 6 *A*). The averaged current amplitude, measured at the end of 2-s depolarizing pulse at test potential of +50 mV, was inhibited to 68.4 ± 7.9% (n = 8) from control (P < 0.001). After switch back to the normal Tyrode's solution, the current magnitude was recovered nearly to the control level.

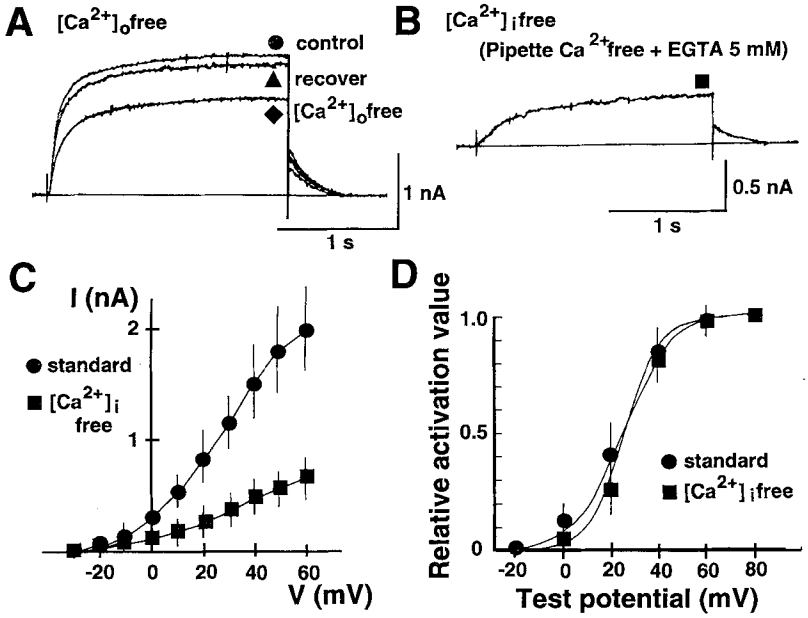

FIGURE 6. Ca^{2+}-sensitivity of the delayed rectifier outward current. (*A*) Effect of external Ca^{2+} on the current. Control trace (*circle*) was recorded in the external normal Tyrode's solution ($[Ca^{2+}]$ = 1.8 mM). Then the external solution was changed to the Ca^{2+}-free solution (0 mM Ca^{2+} with 5 mM EGTA). The current was recorded after 5 min exposure to the Ca^{2+}-free external solution (*diamond*). The external solution was switched back to the normal Tyrode's solution and the current was again recorded after 5 min (*triangle*). The Ca^{2+}-unbuffered internal solution was used for the pipette solution. The current was evoked by 2-s duration of test pulses to +50 mV from the holding potential of −50 mV. (*B*) Effect of internal Ca^{2+} on the current. The current was recorded using the Ca^{2+}-free pipette solution (0 mM Ca^{2+} with 5 mM EGTA) in a different cell. The voltage-clamp pulse was applied same as *A*. Note the smaller elicited current. (*C*) The averaged *I-V* relationships of outward current measured from different cells in different $[Ca^{2+}]_i$; the standard and the Ca^{2+}-free condition. The former was using standard pipette solution ($[Ca^{2+}]$ = 0.1 μM, *circles*). The latter used Ca^{2+}-free pipette solution (0 mM Ca^{2+} with 5 mM EGTA; pCa > 9, *squares*). The vertical bar through each point represents the SD (n = 10 in the standard condition and n = 9 in the Ca^{2+}-free condition). (*D*) The activation curves (P_∞ curves) for the tail current determined at different $[Ca^{2+}]_i$, circles represent the standard condition (pCa = 7) and squares are Ca^{2+}-free condition (pCa > 9). The tail current was measured using 2-s depolarizing pulses from the holding potential of −50 mV. The amplitudes were normalized by the amplitude of the tail current at +80 mV and were plotted as a function of test voltage. Curves were the least-square fit of Eq. 3 in the text. The vertical bar through each point represents the SD (n = 6 in the standard condition and n = 5 in the Ca^{2+}-free condition).

To minimize possible changes in membrane surface charges, the experiment was duplicated using the Ca^{2+}-free high-Mg^{2+} solution. The solution was prepared by replacing external Ca^{2+} to an equivalent concentration of Mg^{2+}. Similar results were obtained using this solution (n = 5, not shown), suggesting that the inhibition was not caused by alteration of membrane surface charges. These results suggest that external Ca^{2+} cannot directly affect the current.

The Ca^{2+} modification on the delayed rectifier outward current was further tested using the Ca^{2+}-free internal solution containing 5 mM EGTA. In this condition, the intracellular free Ca^{2+} concentration ($[Ca^{2+}]_i$) is below 10^{-9} M (pCa > 9) by the prediction of Fabiato and Fabiato (1979). Using this internal solution, delayed rectifier outward current was dramatically inhibited (Fig. 6 *B*). The current amplitude at +50 mV was significantly smaller than that recorded in the standard condition in which standard internal ($[Ca^{2+}]$ = 0.1 μM) pipette solution was used in the external normal Tyrode's solution. The averaged current amplitude was suppressed to 32.2 ± 7.0% (n = 9) from control ($P < 0.001$). The *I-V* curve averaged from nine different cells demonstrated smaller conductance than control (Fig. 6 *C*). When the current was recorded in Ca^{2+}-free internal and external solutions (pCa > 9), the similar level of inhibition was obtained (30.9 ± 8.1% of control, n = 4).

To assess the effect of Ca^{2+} on the voltage-dependence of the current activation, the activation curves (P_∞ curve) for the current were compared between the different $[Ca^{2+}]_i$; $[Ca^{2+}]_i < 10^{-9}$ M (pCa > 9) and $[Ca^{2+}]_i = 1.0 \times 10^{-7}$ M (pCa = 7). The tail current was measured using 2-s depolarizing pulses from holding potential of −50 mV. The relative activation values at various membrane potentials (E) were obtained by normalizing the amplitude of the tail current by the values at +80 mV. The averaged data points were then fitted by Eq. 2. Fig. 6 *D* shows the relative P_∞ curves determined at pCa > 9 and pCa = 7. V_h was 27.5 mV and K was 10.4 mV at pCa > 9, while V_h was 29.1 mV and K was 8.8 mV at pCa = 7. Neither V_h nor K were significantly different between the two different conditions.

These results suggest that $[Ca^{2+}]_i$ affects the delayed rectifier K^+ currents without affecting the voltage dependence of the current activation.

Pharmacological Modification on the Current

4-aminopyridine (4-AP), known to inhibit the voltage-gated delayed rectifier K^+ channel (Ulbricht and Wagner, 1976; Yeh, Oxford, Wu, and Narahashi, 1976; Kenyon and Gibbons, 1979; Bostock, Sears, and Sherratt, 1981; Hermann and Gorman, 1981), was applied to the bath solution to test the effect on the delayed rectifier outward current (Fig. 7 *A*). 4-AP (2 mM) inhibited the current in seven of seven cells tested. The averaged current amplitude at +50 mV was inhibited to 26.7 ± 4.4% of control (n = 7, $P < 0.001$) during exposure to 4-AP and partially recovered following washout of 4-AP. This inhibition was observed at all voltages tested. The averaged *I-V* relationships before, during exposure to and after washout of 4-AP are shown in Fig. 7 *B*. The block was concentration dependent (Fig. 7 *C*). The concentration-dependent inhibition of the current was fitted by the least-squares method to Eq. 3 with the P_{max} setting to 1. The relationship between the concentration of 4-AP and the current amplitude was fitted by the equation with a Hill coefficient of 1. The IC_{50} was 0.21 mM.

In a variety of regions and species, the Ca^{2+}-activated K^+ permeability is inhibited by apamin; a peptide toxin isolated from bee venom (Banks, Brown, Burgess, Burnstock, Claret, Cooks, and Jenkinson, 1979; Burgess, Claret, and Jenkinson, 1981; Hugues, Romey, Duval, Vincent, and Lazdunski, 1982; Cook and Haylett, 1985; Blatz and Magleby, 1986). Fig. 8 shows an example of the effect of externally applied 50 nM apamin on the delayed rectifier outward current. After three min exposure to apamin, the current was suppressed. The extent of inhibition during

exposure to apamin was 46.1 ± 5.8% (n = 8) of control at +50 mV (Fig. 8 *B*). The inhibition by apamin (50 nM) was irreversible during 30 min washout period (n = 6).

Hormonal modification of the delayed rectifier outward current was also examined. The permeability of the hepatocyte plasma membrane to K^+ is increased by α_1-adrenergic receptor stimulation with noradrenaline (Burgess et al., 1979; Field and Jenkinson, 1987; Capiod and Ogden, 1989*a*; Ogden et al., 1990). This response

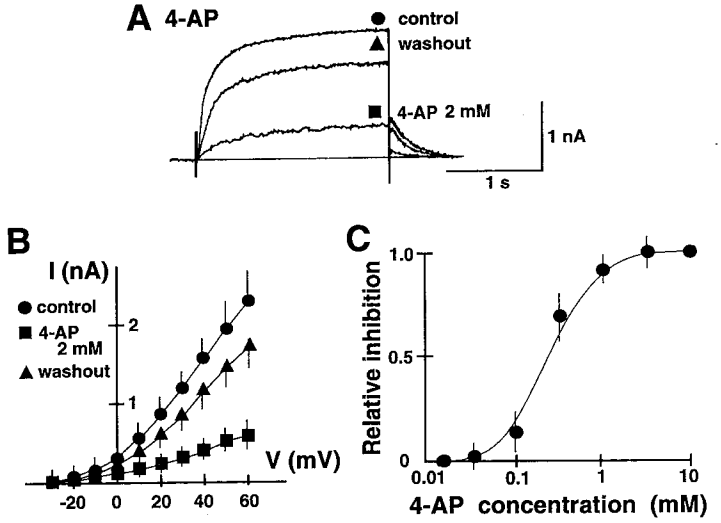

FIGURE 7. Effect of 4-AP on the delayed rectifier outward current. (*A*) Effect of bath application of 4-AP (2 mM) on the outward current at 37°C. The standard internal solution was used for the pipette solution. Following the measurement of the current in the normal Tyrode's solution (*circle; control*), 4-AP (2 mM) was applied to the external solution. The current was measured during exposure to (*squares*) and after washout of 4-AP (*triangles*). The current was evoked by 2-s duration of test pulses to +50 mV from a holding potential of −50 mV. Magnitude of the current was decreased following application of 4-AP. (*B*) The *I-V* relationships of the current in control (*circles*), during exposure to (*squares*) and after washout of 4-AP (*triangles*). The vertical bar through each point represents the SD (n = 7 for each). (*C*) Concentration-dependent inhibition of the outward current by 4-AP. The graph shows the relationship between the relative inhibition of the current and the concentration of 4-AP obtained from five different cells. The continuous line is a curve fit to Eq. 3. The relative inhibition was obtained from normalizing the inhibited current value to the maximum inhibition at 10 mM. The Hill coefficient of the fitted curve was 1 and the half-maximal inhibition (IC_{50}) was 0.21 mM.

is due to an increase in $[Ca^{2+}]_i$ (Weiss and Putney, 1978; Burgess et al., 1979; for review see Berridge and Irvine, 1984; Burgess, Godfrey, McKinney, Berridge, Irvine, and Putney, 1984; Burgess, Irvine, Berridge, McKinney and Putney, 1984; Ogden et al., 1990). The effect of noradrenaline on the delayed rectifier outward current was examined (Fig. 9 *A*). To eliminate the noradrenaline-induced Cl^- conductance, Cl^--free internal and external solutions were used. Bath application of noradrenaline (1 μM) reversibly enhanced the delayed rectifier outward current with increasing the

conductance. The enhancement of the current was observed in both Ca^{2+}-containing and Ca^{2+}-free external solutions (n = 6 for each). However, the net effect on the delayed rectifier current is unknown, because it is likely that the previously reported $I_{K(Ca)}$ contaminates this current increase. In contrast to noradrenaline, β-adrenergic stimulation with isoproterenol (1 μM) did not cause any effects on the outward current (Fig. 9 *B*). Similar results were obtained in nine other cells (0.1–10 μM). The averaged *I-V* relationship before and during exposure to isoproterenol (1 μM) were almost superimposed (Fig. 9 *B, bottom*). In addition, neither bath application of forskolin (10 μM) nor internal application (to the pipette solution) of cAMP (10 μM) modulated the current (n = 4 for each, not shown). Effects of other hormones, glucagon (0.1–1 μM) and insulin (0.05–0.1 U/ml), were also tested on the current, but they failed to affect the current (n = 4 for each).

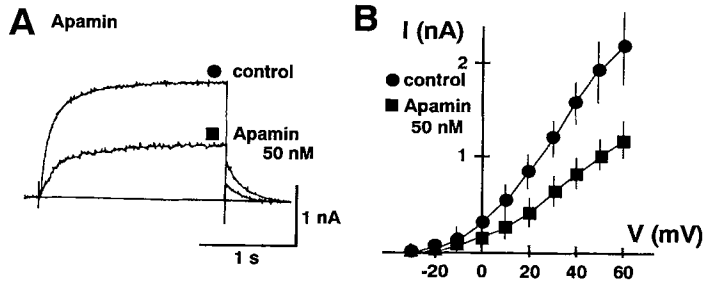

FIGURE 8. Modification of the delayed rectifier outward current by apamin. (*A*) Effect of bath application of apamin (50 nM) on the outward current. After the measurement of the current (*circle; control*) in the normal Tyrode's solution, apamin (50 nM) was applied to the external solution at 37°C. The standard internal solution was used for the pipette solution. Five min after the application, the current was again measured (*squares*). The current was evoked by 2-s duration of test pulses to +50 mV from a holding potential of −50 mV. Magnitude of the current was inhibited following application of apamin. (*B*) The *I-V* relationships of the current in control (*circles*) and during exposure to apamin (*squares*). The vertical bar through each point represents the SD (n = 8 for each).

Voltage-gated Single-Channel Current in Outside-out Patches

To investigate the characteristics of channel gating and modification of the current by intracellular Ca^{2+} in more detail, single channel currents were measured in excised outside-out and inside-out patch configurations.

Fig. 10 *A* shows examples of single channel activity recorded in the outside-out patch configuration. 2-s duration of test pulses were applied to +50 mV from holding potential of −80 mV. No channel activity was detected at −80 mV, which was close to the K^+ equilibrium potential (E_K). The depolarizing voltage steps to +50 mV caused multiple channel openings after a latency period. Channel activity exhibited bursting behavior. The channel open events in the individual patch increased with time resulted in the enhancement of open channel activity. In contrast, neither unitary current amplitude nor mean open lifetime during the voltage-clamp step changed significantly. Channel open probability (P_o) calculated in the initial 1 s during 2-s voltage-clamp step was 0.64 ± 0.05 (n = 20) and that in the last 1 s was 0.66 ± 0.07

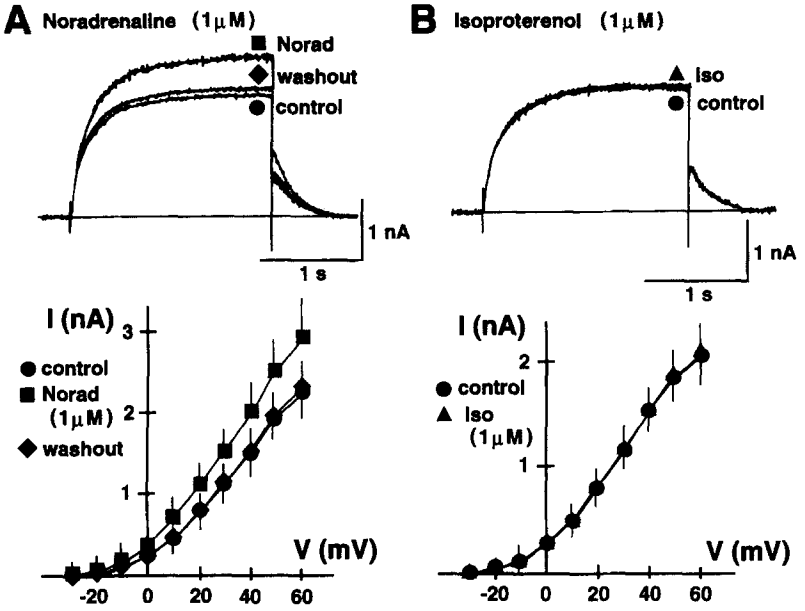

FIGURE 9. Effects of noradrenaline and isoproterenol on the delayed rectifier outward current. (*A, top*) Effect of bath application of noradrenaline (1 μM) on the outward current at 37°C. The Cl^--free internal solution without EGTA was used for the pipette solution. After the measurement of the current in the Cl^--free external solution (*circle; control*), noradrenaline (1 μM) was applied to the external solution. The current was measured during exposure to noradrenaline (squares). After washout of noradrenaline from the bath, the current was recovered nearly to the control level (*diamonds*). The current was evoked by 2-s duration of test pulses to +50 mV from a holding potential of −50 mV. The current magnitude was increased following application of noradrenaline. (*A, bottom*) The *I-V* relationships of the current in control (*circles*), during exposure to (*squares*) and after washout (*diamonds*) of 1 μM noradrenaline. The vertical bar through each point represents the SD (n = 6 for each). (*B, top*) Effect of bath application of isoproterenol (1 μM) on the outward current at 37°C. The standard internal solution was used for the pipette solution. After the measurement of the current in the normal Tyrode's solution (*circle; control*), isoproterenol (1 μM) was applied to the external solution. The current was measured during exposure to isoproterenol (*triangle*). The voltage-clamp pulse was applied same as *A*. The current magnitude was unchanged following application of isoproterenol. (*B, bottom*): The *I-V* relationships of the current in control (*circles*) and during exposure to 1 μM isoproterenol (*triangles*). The two curves were almost superimposed. The vertical bar through each point represents the SD (n = 5 for each).

(n = 20). These values were not different significantly, suggesting that the enhancement of channel activity was caused by either increasing individual burst duration or increasing the channel number being open. Unitary amplitude changed according to the different voltage steps and no inward-directed current was detected in voltage steps negative to E_K. The ensemble averaged current was given in Fig. 10 *A, bottom,* which was obtained from 150 consecutive sweeps at +50 mV. The ensemble current demonstrated the time-dependent increase in current amplitude. The increase of the ensemble current was best described by a double exponential function with a time constant for the fast phase of 97.5 ± 18.2 ms and that for the slow phase of 1010 ±

237 ms (n = 4). The ratio of the current during the pulse to the tail current was 2.34 ± 0.20 (n = 4). These characteristics were consistent with those obtained in whole-cell measurements.

Frequency distributions of the unitary current amplitudes were fit with a Gaussian curve (Fig. 10 *B*). The mean current amplitude for the channel was 0.96 ± 0.11 pA

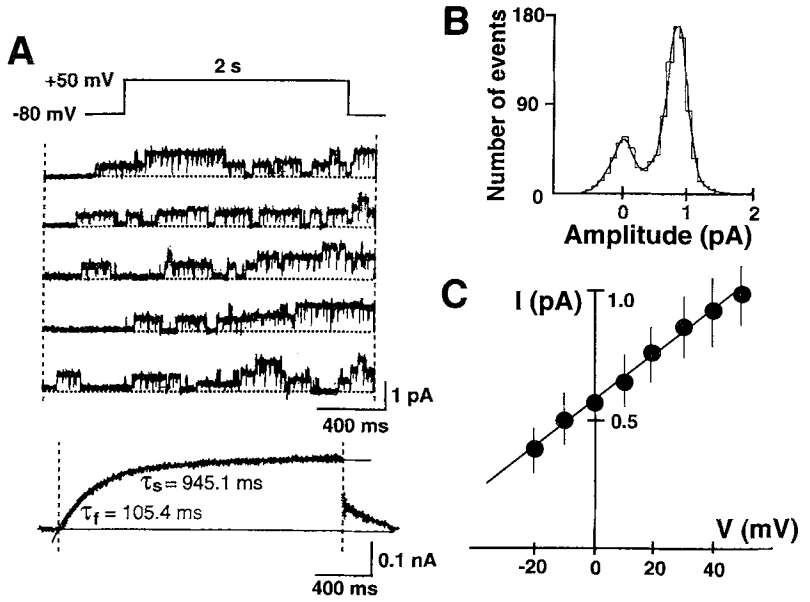

FIGURE 10. The delayed rectifier outward current measured by outside-out patch single channel recordings. (*A, top*) Sequential sweeps were sampled during 2-s voltage-clamp steps to +50 mV from a holding potential of −80 mV in the normal Tyrode's solution at 37°C. The pipette solution was the standard internal ($[Ca^{2+}]$ = 0.1 μM). The leak and capacitative currents have been subtracted in all sweeps. The outward-directed channel activity was evoked with latency period. The dotted line running in each trace indicates the closed state (baseline level). This patch contains at least three channels. Data were recorded with low-pass filtering at 2 KHz and digitized at 10 KHz. (*A, bottom*) The ensemble averaged current obtained from 150 consecutive sweeps at +50 mV. The smooth line in the averaged current indicates fitting of a least-square routine. The time-dependent increase of the ensemble current was best described by a double exponential function with a time constant for the fast phase of 105.4 ms and that for the slow phase of 945.1 ms. (*B*) The frequency distribution of the current amplitude at +50 mV formed from the different cell which contained one channel activity. The amplitude of the channel was 0.95 pA at +50 mV. The ordinate gives the number of events and the abscissa is the current amplitude. The distribution is fit with a Gaussian function. (*C*) The averaged single channel *I-V* relationship plotted from five different cells. Slope conductance is 9.3 pS in the 5.4 mM K^+ in the bath solution.

(n = 5) at +50 mV. Fig. 10 *C* shows the averaged single channel *I-V* relationship. Straight line could be drawn in the voltage range between −20 and +50 mV with a slope conductance of 9.5 ± 2.2 pS (n = 10) at 37°C. The ratio of the current during the pulse to the tail current was constant in this voltage range, indicating that the *I-V* curve of the tail current is also linear.

Fig. 11 shows the distribution of open and closed times of the channel at +50 mV. Open time distribution was best described by a single exponential function with the mean open lifetime of 18.5 ± 2.6 ms (n = 14, Fig. 11 *A*, *top*). The mean open lifetime exhibited weak voltage dependence; the value became smaller with membrane hyperpolarization (Fig. 11 *A*, *bottom*). In contrast, at least two exponentials were

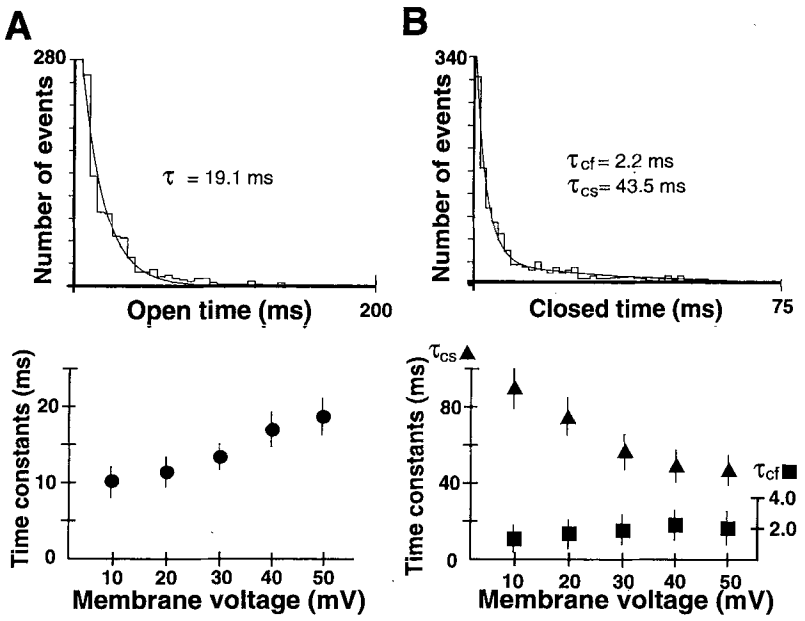

FIGURE 11. Dwell time histograms and the voltage dependence of the dwell time constants of single delayed rectifier outward current in outside-out patch recordings. (*A*, *top*) Histogram of open times recorded from a representative single channel at +50 mV. This patch never exhibited more than a single channel during 220 of consecutive sweeps. Open times, recorded with low-pass filtering at 2 KHz, were segregated into 5-ms bins. Open state lifetimes were distributed according to a single exponential function with a time constant (τ_o) of 19.1 ms. (*A*, *bottom*) The voltage-dependence of the mean open lifetime. The mean open lifetime (*circles*) was plotted as a function of test voltage. The vertical bar through each point represents the SD (n = 5). (*B*, *top*) Closed times histogram determined at +50 mV. The initial latency period of each sweep was omitted in constructing the histogram. Bin duration was 1.5 ms. At least two exponentials were required to fit the closed time distributions with time constants of 2.2 ms for the fast component (τ_{cf}) and 43.5 ms for the slow component (τ_{cs}). (*B*, *bottom*) The voltage-dependence of the mean closed times. Mean closed times (τ_{cf}; *squares*, and τ_{cs}; *triangles*) were plotted as a function of test voltage. The vertical bar through each point represents the SD (n = 5).

required to fit the closed time distributions with a time constant for the fast component of 2.0 ± 0.3 ms (n = 14) and that for the slow component of 47.7 ± 5.9 ms (n = 14, Fig. 11 *B*, *top*). Time constants for slow component plotted against membrane voltage also exhibited voltage-dependence, but that for the fast component did not (Fig. 11 *B*, *bottom*).

Ca^{2+}-sensitive Nature of the Single-Channel Current in Inside-out Patches

Modification of the delayed rectifier outward current by intracellular Ca^{2+} was estimated directly using excised inside-out patch recordings. Single-channel activity was measured in different [Ca^{2+}] of bath solution (cytosolic side of the membrane) at a test voltage of +50 mV. Fig. 12 *A* shows examples recorded in different bath solutions. Channel activity was influenced by Ca^{2+} in the bath. Channel open probability (P_o) became greater with increasing [Ca^{2+}] in the bath solution. In contrast, neither the mean open lifetime nor unitary current amplitude was affected. The mean open lifetime was 17.9 ± 2.4 ms (n = 5) recorded at 0.01 μM Ca^{2+}

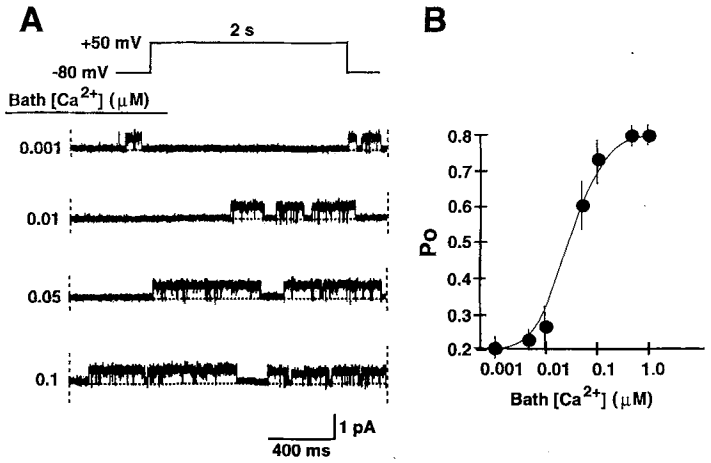

FIGURE 12. Ca^{2+}-dependence of the single channel delayed rectifier outward current in inside-out patch recordings. (*A*) Sequential sweeps were sampled during 2-s voltage-clamp steps to +50 mV from the holding potential of −50 mV. Bath solutions (cytosolic side of the membrane) with various concentrations of Ca^{2+} ($[Ca^{2+}]_i$) were applied at 37°C. $[Ca^{2+}]_i$ is indicated to the left of each current sweep. The leak and capacitative currents have been subtracted in all sweeps. Data were recorded with low-pass filtering at 2 KHz and digitized at 10 KHz. (*B*) $[Ca^{2+}]_i$ concentration-dependent change of channel open probability (P_o) of the outward current. The graph shows the relationship between P_o of the channel and $[Ca^{2+}]_i$ from six different cells. The continuous line is a curve fit by Eq. 3. The Hill coefficient of the fitted curve was 1 and the half-maximal inhibition (IC_{50}) was 0.031 μM.

solution and 18.6 ± 2.9 ms (n = 5) at 0.1 μM Ca^{2+} solution. Channel activity continued even in solutions containing less than 10^{-9} M of Ca^{2+}. Fig. 12 *B* illustrates the Ca^{2+} concentration dependence of the channel. P_o at each concentration of Ca^{2+} was estimated. The concentration-dependent activation of the current was fitted by the least-squares method to Eq. 3. The relationship between [Ca^{2+}] and the channel activity was fitted by the equation with a Hill coefficient of 1 for the channel. The IC_{50} was 0.031 μM.

DISCUSSION

The major findings in this study are as follows: (*a*) at physiological temperature (~37°C), the delayed rectifier outward K^+ current was found in enzymatically

isolated guinea pig hepatocytes; (*b*) the growth of the tail current in the envelope test followed that of the activation. The time course of growth and deactivation of the tail current were best described by a sum of two exponentials; (*c*) Intracellular Ca^{2+} modulates the currents without affecting the voltage-dependence of the current activation; (*d*) the current was suppressed by external application of 4-AP or apamin; (*e*) single-channel activity exhibited time- and voltage-dependent nature whose ensemble averaged current was consistent with whole-cell current measurements; and (*f*) channel activity in inside-out patch configurations demonstrated a Ca^{2+}-dependent change in open probability. These results indicate that guinea pig hepatocytes possess voltage-gated delayed rectifier K^+ channels which are modulated by intracellular Ca^{2+}.

Relation to Previous Electrophysiological Studies

Previous studies in guinea pig hepatocyte plasma membranes showed Ca^{2+}-activated K^+ permeability which is sensitive to α_1-adrenergic stimulation and is inhibited by apamin (Burgess et al., 1981; Capiod et al., 1987; Field and Jenkinson, 1987; Capiod and Ogden, 1989*a*). Recently, Capiod and Ogden (1989*b*) demonstrated the single $I_{K(Ca)}$ channel activity. However, their reported $I_{K(Ca)}$ in guinea pig hepatocytes appears to be different from our described delayed rectifier channel. $I_{K(Ca)}$ observed by Capiod and Ogden (1989*b*) exhibited neither time- nor voltage-dependent nature; the inward directed current was observed at potentials negative to the K^+ equilibrium potential (E_K); the single-channel slope conductance was 6 pS at physiological K^+ concentrations; and channel activation occurred in $[Ca^{2+}]_i$ range of 0.3–1.0 μM and the channel was completely inactive at $[Ca^{2+}]_i$ lower than 0.3 μM. Different from these characteristics, our described delayed rectifier K^+ channel exhibited only outward conductance with single-channel slope conductance (9.5 pS) greater than $I_{K(Ca)}$. In addition, our described channel was sensitive to much lower $[Ca^{2+}]_i$ range than $I_{K(Ca)}$; the current was active at pCa > 9 and almost saturated at ~0.3 μM (IC_{50} of 0.031 μM).

The membrane ionic currents in guinea pig hepatocytes described in previous studies exhibited no time-dependent delayed rectifier properties. Majority of these previous studies were likely to be performed at relatively low temperature (~20–30°C). Although we did not examine the temperature-dependent property of the delayed rectifier current in detail, the current appears to be sensitive to the temperature and inactivated at room temperature (~20°C). This evidence is consistent with the report by Kolb and Adam (1976); in isolated hepatocytes, cellular K^+ content at 37°C is greater than that at 25°C, when $[Ca^{2+}]_o$ is in the normal range of 0.5–1.2 mM. The temperature-dependent property of the delayed rectifier K^+ channel has been shown in cardiac myocytes; the amplitude of the current is much smaller at room temperature than at ~37°C (Walsh, Begenisich, and Kass, 1988, 1989). Recently, cell volume-sensitive K^+ conductance has been shown in guinea pig hepatocytes (Sandford, Sweiry, and Jenkinson, 1992). However, the channel opening is not mediated by internal Ca^{2+}. In rat hepatocytes, the outward K^+ conductance (Burgess et al., 1981) and inwardly-rectifying K^+ channel (Henderson et al., 1989) have been reported. Both of these currents were Ca^{2+} insensitive. Time-dependent delayed rectifier K^+ current was described in isolated avian hepatocytes but the

current was neither sensitive to Ca^{2+} nor inhibited by apamin (Marchetti et al., 1988). In addition, the current was fully activated in 200 ms of depolarizing test pulses. According to these previous reports and our results, the channel described in the present study may be different from previously reported K^+ channels in hepatocytes. Our described channel was sensitive to membrane voltage and intracellular Ca^{2+}. However, the channel remained active in Ca^{2+}-free conditions. In addition, the voltage dependence of the activation curve of the delayed rectifier current was unaffected by $[Ca^{2+}]_i$ in this study. These results suggest that our described channel may not belong to the class of $I_{K(Ca)}$. However, because channel characteristics were evaluated in the different experimental conditions between previous studies and the present study, further study is needed to evaluate in this point.

The voltage-gated delayed rectifier K^+ channel has been described in variety of regions in many species (Noble and Tsien, 1969; McDonald and Trautwein, 1978; Adams, Brown, and Constanti, 1982; Okabe, Kitamura, and Kuriyama, 1987; Hume and Leblanc, 1989; Tohse, 1990; Bonnet, Rusch, and Harder, 1991). Among them, the channel described in the present study shows several similarities to the channel reported in smooth muscle cells from rabbit pulmonary artery (Okabe et al., 1987). The channel in smooth muscle cell exhibits both Ca^{2+}-sensitive and the voltage-gated delayed rectifier nature. The channel is also sensitive to 4-AP. In contrast, the channel sensitivity to apamin is unclear. In addition, the IC_{50} of 4-AP inhibition of the channel is relatively larger than that in our described channel.

The delayed rectifier K^+ channel in cardiac myocytes is known to be enhanced by β-adrenergic stimulation via cyclic AMP-dependent protein kinase (PKA)-induced phosphorylation (Tsien, Giles, and Greengard, 1972; Brown and Noble, 1974; Bennett, McKinney, Begenisich, and Kass, 1986; Walsh et al., 1989). The channel, in this study, had no response to isoproterenol, forskolin or cAMP, suggesting that the channel is not modulated by phosphorylation.

Gating Kinetics of the Channel

The gating behavior of the delayed rectifier K^+ channel described here resembles that in previously reported in cardiac preparations (Gintant, Datyner, and Cohen, 1985; Bennett, McKinney, Begenisich, and Kass, 1985). The activation and deactivation time courses of whole-cell current were well described by a double exponential function. The voltage-dependent activation curve was well fitted by a Boltzmann distribution. It is unlikely that the biexponential kinetics of the activation and inactivation are caused by two distinct population of the channel, because single channel recordings exhibited uniform currents at all test voltages and open time distribution was best described by a single exponential function. These results from single channel data suggest that only one population of channel activity produces the time- and voltage-dependent activation. The identification of unitary current was based on the following results: (*a*) the ensemble averaged current from consecutive single channel sweeps reproduced the macroscopic current, whose activation time course was best described by a double exponential function. The time constants were similar to those obtained from whole-cell measurements; (*b*) single-channel activity was not observed at estimated E_K of ~ -80 mV, and (*c*) single-channel slope conductance was ~ 10 pS, which was similar to that of the delayed rectifier K^+

channel reported previously in other species or in other systems (Clapham and Logothetis, 1988; Marchetti et al., 1988; Balser, Bennett, and Roden, 1990). Single-channel measurements provided time- and voltage-dependent channel behavior similar to those observed in whole-cell experiments.

Single-channel behavior exhibited open bursting behavior separated by interburst periods. Although neither the mean open lifetime nor shut period during a burst showed significant voltage dependence, shut periods between bursts increased with less depolarization of the membrane voltage. According to the dwell time histograms of open and closed time distributions, channel state can be described by a linear sequential gating scheme having one open and two closed states:

$$C_1 \underset{k-1}{\overset{k+1}{\rightleftharpoons}} C_2 \underset{\alpha}{\overset{\beta}{\rightleftharpoons}} O$$

SCHEME I

where C_1 and C_2 are closed states, O is the open state, $k + 1$ and $k - 1$ are rate constants between C_1 and C_2 states and α and β are rate constants between C_2 and O

TABLE I

Voltage-dependence of the Rate Constants

Voltage	α	β	$k - 1$	$k + 1$
mV				
+50	54.6 ± 4.8	424.1 ± 57.0	58.9 ± 6.7	17.6 ± 6.7
+30	76.7 ± 5.8	469.5 ± 61.1	59.1 ± 5.7	15.2 ± 4.9
+10	96.4 ± 7.5	851.0 ± 79.3	122.7 ± 9.9	8.9 ± 3.8
−10	127.4 ± 10.8	840.0 ± 76.5	149.5 ± 11.2	1.6 ± 0.7

Rate constants were calculated in terms of a linear sequential gating scheme ($C_1 - C_2 - O$) at different test potentials between +50 and −10 mV. α and β are rate constants (s^{-1}) between C_2 and O states and $k + 1$ and $k - 1$ are rate constants (s^{-1}) between C_1 and C_2 states. All rate constants were expressed as mean ± SD from 12 different outside-out patches.

states. Each rate constant was calculated from a function of the dwell time constants and open probability at the given voltage using the two closed states gating scheme (Colquhoun and Hawkes, 1981). Averaged rate constants at +50 mV from 12 different patches were $\alpha = 54.6 \pm 4.8$, $\beta = 424.1 \pm 57.0$, $k - 1 = 58.9 \pm 6.7$, $k + 1 = 17.6 \pm 6.7$ s^{-1}. Table I summarizes the rate constants in different test voltages between +50 and −10 mV. Decreasing the rate constant of $k + 1$ appears to be responsible for the voltage-dependent increase of the time constant for the slow component of closed time distributions which would cause the prolongation of the closed period and decrease of channel P_o (Fig. 11). By using these rate constants, the probability density function to describe apparent burst behavior was obtained (Eq. 2.22) in Colquhoun and Hawkes, 1981) and the mean apparent burst length was calculated as 192.8 ± 40.7 ms ($n = 12$) at +50 mV. Individual bursts contain 6–11 open events interspersed with brief shut periods. Table II summarizes the comparison between the observed (experimental) and the predicted burst length calculated using the rate constants in Table I in voltages between +50 and −10 mV. They were

TABLE II

Comparison of the Observed (Experimental) and Predicted Burst Lengths at Different Voltages

Voltage	Observed burst length	Predicted burst length
mV	*ms*	*ms*
+50	228.5 ± 37.0	192.8 ± 40.7
+30	177.4 ± 29.1	154.0 ± 36.1
+10	131.2 ± 27.1	108.5 ± 24.7
−10	92.5 ± 24.4	72.2 ± 16.3

The observed burst length was averaged from five different outside-out patches. The predicted burst length was calculated from rate constants shown in Table I (n = 12). Data were expressed as mean ± SD. No significant differences were detected between the two values in each voltage.

not different significantly at each test voltage. The close agreement between the experimental and the predicted burst length supports the linear sequential gating scheme with two closed states and single open state. Similar multistate linear sequential gating scheme has been used to characterize the kinetics of the delayed rectifier channel in other systems (Conti and Neher, 1980; Young and Moore, 1981; Gintant et al., 1985).

The burst length appears to be sensitive to $[Ca^{2+}]_i$. The observed burst length was longer at higher $[Ca^{2+}]_i$; it was 100.7 ± 23.5 ms at 0.001 μM, 175.1 ± 26.3 ms at 0.01 μM and 182.5 ± 26.9 ms at 0.1 μM in inside-out patch recordings (n = 5). Table III summarizes the dependence of the burst length (the observed and predicted burst lengths) on $[Ca^{2+}]_i$ at +50 mV in excised inside-out configurations. Burst length at $[Ca^{2+}]_i$ = 0.001 μM was significantly shorter than that at $[Ca^{2+}]_i$ = 0.1 μM. Therefore, burst length appears to be responsible for increasing P_o value at higher $[Ca^{2+}]_i$.

Physiological Implications

The delayed rectifier K^+ channel in cardiac cell membranes appears to be important in determining the membrane repolarization of the action potentials (McDonald and Trautwein, 1978; Hume and Uehara, 1985). In guinea pig hepatocytes, the resting

TABLE III

Comparison of the Observed (Experimental) and Predicted Burst Lengths at Different $[Ca^{2+}]_i$

$[Ca^{2+}]_i$	Observed burst length	Predicted burst length
μM	*ms*	*ms*
0.001	100.7 ± 23.5*	81.3 ± 12.4*
0.01	175.1 ± 26.3	181.5 ± 24.0
0.1	182.5 ± 26.9	190.7 ± 49.0

The observed burst length was averaged from five different inside-out patches at −50 mV. The predicted burst length was calculated from 4–5 different inside-out patches. Data were expressed as mean ± SD. No significant differences were detected between the two values.

*$P < 0.05$ different from the values at $[Ca^{2+}]_i$ = 0.01 and 0.1 μM.

membrane potential is positive to E_K, suggesting that the hepatocyte membrane have a relatively high resting Na^+ and Cl^- permeability (P_{Na} and P_{Cl}) compared to cardiac cell membrane. Enhancement of these resting ion permeabilities have been shown in rat hepatocytes (Graf, Henderson, Krumpholz, and Boyer, 1987). The resting membrane potential in isolated guinea pig hepatocyte was ~ -25 mV, while the membrane voltage of the delayed rectifier K^+ current activation is ~ -20 mV. The closeness between the resting membrane potential and the current activation voltage suggests that the current activates when the membrane is depolarized positive to ~ -20 mV. Membrane depolarization may trigger the current activation even normal level of $[Ca^{2+}]_i$; any agent that causes a membrane depolarization may trigger the current activation. This may represent a negative feedback control on the membrane potential. Ca^{2+}-mobilizing hormones causes the rise of $[Ca^{2+}]_i$ and the elevated $[Ca^{2+}]_i$ can enhance the current magnitude without affecting the activation kinetics.

In physiological solutions, the mean whole-cell current amplitude at 0 mV was ~ 0.31 nA. Because the mean calculated cell capacitance was 31.4 pF, the current amplitude can be estimated as ~ 10 pA/pF. The net whole-cell current magnitude at 0 mV was similar to that in the delayed rectifier K^+ current in avian hepatocytes (~ 14 pA/pF at 0 mV) measured at 140 mM K^+ inside and 5.4 mM K^+ outside (Marchetti et al., 1988). These estimations suggest that the outward K^+ conductance through the delayed rectifier K^+ channel may, at least in part, play a role to prevent membrane depolarization.

Finally, the delayed rectifier K^+ current is operative in the physiological range of $[Ca^{2+}]_i$. The resting level of $[Ca^{2+}]_i$ is 0.1–0.2 μM in hepatocytes (Orrenius, Nicotera, and Bellomo, 1989; Ogden et al., 1990). At this level of $[Ca^{2+}]_i$, the previously reported $I_{K(Ca)}$ is completely inactive, because $I_{K(Ca)}$ requires $[Ca^{2+}]_i$ higher than 0.3 μM to activate (Capiod and Ogden, 1989*b*). Before activation of $I_{K(Ca)}$, the delayed rectifier K^+ current may contribute to maintain the resting membrane potential.

The authors wish to thank Dr. Robert G. Tsushima and Dr. Ana-Maria Vites (Department of Medicine, Northwestern University) for valuable comments on the manuscript, and Dr. H. Seno (Department of Physiology, Nippon Medical School) for providing a computer program for data acquisition and analysis.

Original version received 18 October 1993 and accepted version received 22 February 1994.

REFERENCES

Adams, P. R., D. A. Brown, and A. Constanti. 1982. M-currents and other potassium currents in bullfrog sympathetic neurons. *Journal of Physiology.* 330:537–572.

Banks, B. E. C., C. Brown, G. M. Burgess, G. Burnstock, M. Claret, T. M. Cooks, and D. H. Jenkinson. 1979. Apamin blocks certain neurotransmitter induced increases in potassium permeability. *Nature.* 282:415–417.

Balser, J. R., P. B. Bennett, and D. M. Roden. 1990. Time-dependent outward current in guinea pig ventricular myocytes. Gating kinetics of the delayed rectifier. *Journal of General Physiology.* 96:835–863.

Bear, C. E., and O. H. Petersen. 1987. L-alanine evokes opening of single Ca^{2+}-activated K^+ channels in rat liver cells. *Pflügers Archiv.* 410:342–344.

Bennett, P. B., L. McKinney, T. Begenisich, and R. S. Kass. 1986. Adrenergic modulation of the delayed rectifier potassium channel in calf cardiac Purkinje fibers. *Biophysical Journal.* 49:839–848.

Bennett, P. B., L. McKinney, R. S. Kass, and T. Begenisich. 1985. Delayed rectification in the calf cardiac Purkinje fiber. Evidence for multiple state kinetics. *Biophysical Journal.* 48:553–567.

Berridge, M. J., and R. F. Irvine. 1984. Inositol triphosphate, a novel second messenger in cellular signal transduction. *Nature.* 312:315–321.

Blatz, A. L., and K. L. Magleby. 1986. Single apamin-blocked Ca-activated K^+ channels of small conductance in cultured rat skeletal muscle. *Nature.* 323:718–720.

Bonnet, P., N. J. Rusch, and D. R. Harder. 1991. Characterization of an outward K^+ current in freshly dispersed cerebral arterial muscle cells. *Pflügers Archiv.* 418:292–296.

Bostock, H., T. A. Sears, and R. M. Sherratt. 1981. The effects of 4-aminopyridine and tetraethylammonium ions on normal and demyelinated mammalian nerve fibers. *Journal of Physiology.* 313:301–315.

Brown, H. F., and S. J. Noble. 1974. Effects of adrenaline on membrane currents underlying pacemaker activity in frog atrial muscle. *Journal of Physiology.* 238:51–53P.

Burgess, G. M., M. Claret, and D. H. Jenkinson. 1979. Effects of catecholamines, ATP and ionophore A23187 on potassium and calcium movement in isolated hepatocytes. *Nature* 279:544–546.

Burgess, G. M., M. Claret, and D. H. Jenkinson. 1981. Effects of quinidine and apamin on the calcium-dependent potassium permeability of mammalian hepatocytes and red cells. *Journal of Physiology.* 317:67–90.

Burgess, G. M., P. P. Godfrey, J. S. McKinney, M. J. Berridge, R. F. Irvine, and J. W. Putney, Jr. 1984. The second messenger linking receptor activation to initial Ca^{2+} release in liver. *Nature.* 309:63–66.

Burgess, G. M., R. F. Irvine, M. J. Berridge, J. S. McKinney, and J. W. Putney, Jr. 1984. Actions of inositol phosphates on Ca^{2+} pools in guinea-pig hepatocytes. *Biochemical Journal.* 224:741–746.

Capiod, T., and D. C. Ogden. 1989*a*. Properties of membrane ion conductances evoked by hormonal stimulation of guinea-pig and rabbit isolated hepatocytes. *Proceedings of the Royal Society of London B. Biological Sciences.* 236:187–201.

Capiod, T., and D. C. Ogden. 1989*b*. The properties of calcium-activated potassium ion channels in guinea-pig isolated hepatocytes. *Journal of Physiology.* 409:285–295.

Capiod, T., A. C. Field, D. C. Ogden, and C. A. Sandford. 1987. Internal perfusion of guinea-pig hepatocytes with buffered Ca^{2+} or inositol 1,4,5-triphosphate mimics noradrenaline activation of K^+ and Cl^- conductances. *FEBS Letters.* 217:245–252.

Clapham, D. E., and D. E. Logothetis. 1988. Delayed rectifier K^+ current in embryonic chick heart ventricle. *American Journal of Physiology.* 254:H192–H197.

Colquhoun, D., and A. G. Hawkes. 1981. On the stochastic properties of single ion channels. *Proceedings of the Royal Society of London B. Biological Sciences.* 211:205–235.

Colquhoun, D., and F. J. Sigworth. 1983. Fitting and statistical analysis of single-channel records. *In* Single-Channel Recording. B. Sakmann and E. Neher, editors. Plenum Publishing Corp., NY. 191–263.

Conti, F., and E. Neher. 1980. Single channel recordings of K^+ currents in squid axons. *Nature.* 285:140–143.

Cook, N. S., and D. G. Haylett. 1985. Effect of apamin, quinine and neuromuscular blockers on Ca^{2+}-activated K^+ channels in guinea-pig hepatocytes. *Journal of Physiology.* 358:373–394.

DeWitt, L. M., and J. M. Putney. 1984. α-adrenergic stimulation of K^+ efflux in guinea-pig hepatocytes may involve Ca^{2+} influx and Ca^{2+} release. *Journal of Physiology.* 346:395–407.

Fabiato, A., and F. Fabiato. 1979. Calculator programs for computing the composition of the solutions containing multiple metals and ligands used for experiments in skinned muscle cells. *Journal de Physiologie.* 75:463–505.

Field, A. C., and D. H. Jenkinson. 1987. The effect of noradrenaline on the ion permeability of

isolated mammalian hepatocytes, studied by intracellular recording. *Journal of Physiology.* 392:493–512.

Gautam, A., O. C. Ng, and J. L. Boyer. 1987. Isolated rat hepatocyte couplets in short-term culture: structural characteristics and plasma membrane reorganization. *Hepatology.* 7:216–223.

Gintant, G. A., N. B. Datyner, and I. S. Cohen. 1985. Gating of delayed rectification in acutely isolated canine cardiac Purkinje myocytes; evidence for a single voltage-gated conductance. *Biophysical Journal.* 48:1059–1064.

Graf, J., J. A. Gautam, and J. L. Boyer. 1984. Isolated rat hepatocyte couplets: a primary secretory unit for electrophysiologic studies of bile secretory function. *Proceedings of the National Academy of Sciences, USA.* 81:6516–6520.

Graf, J., R. M. Henderson, B. Krumpholz, and J. L. Boyer. 1987. Cell membrane and transepithelial voltages and resistances in isolated rat hepatocyte couplets. *Journal of Membrane Biology.* 95:241–254.

Graf, J., and O. H. Peterson. 1978. Cell membrane potential and resistance in liver. *Journal of Physiology.* 284:105–126.

Hamill, O. P., A. Marty, E. Neher, B. Sakmann, and F. J. Sigworth. 1981. Improved patch-clamp technique for high resolution current recording from cell and cell-free membrane patches. *Pflügers Archiv.* 391:85–100.

Haylett, D. G. 1976. Effects of sympathomimetic amines on ^{45}Ca efflux from liver slices. *British Journal of Pharmacology.* 57:158–160.

Haylett, D. G., and D. H. Jenkinson. 1972*a*. Effects of noradrenaline on potassium efflux, membrane potential and electrolyte levels in tissue slices prepared from guinea-pig liver. *Journal of Physiology.* 225:721–750.

Haylett, D. G., and D. H. Jenkinson. 1972*b*. The receptors concerned in the actions of catecholamines on glucose release, membrane potential and ion movements in guinea-pig liver. *Journal of Physiology.* 225:751–772.

Henderson, R. M., J. Graf, and J. L. Boyer. 1989. Inward-rectifying potassium channels in rat hepatocytes. *American Journal of Physiology.* 256:G1028–G1035.

Hermann, A., and A. L. F. Gorman. 1981. Effects of 4-aminopyridine on potassium currents in a molluscan neuron. *Journal of General Physiology.* 78:63–86.

Hugues, M., G. Romey, D. Duval, J.-P. Vincent, and M. Lazdunski. 1982. Apamin as a selective blocker of the calcium-dependent potassium channel in neuroblastoma cells: voltage-clamp and biochemical characterization of the toxin receptor. *Proceedings of the National Academy of Sciences, USA.* 79:1308–1312.

Hume, J. R., and N. Leblanc. 1989. Macroscopic K^+ currents in single smooth muscle cells of the rabbit portal vein. *Journal of Physiology.* 413:49–73.

Hume, J. R., and A. Uehara. 1985. Ionic basis of the different action potential configurations of single guinea-pig atrial and ventricular myocytes. *Journal of Physiology.* 368:525–544.

Kenyon, J. L., and W. R. Gibbons. 1979. 4-Aminopyridine and early outward current of sheep cardiac Purkinje fibers. *Journal of General Physiology.* 73:139–157.

Kolb, H.-A., and G. Adam. 1976. Regulation of ion permeabilities of isolated rat liver cells by external calcium concentration and temperature. *Journal of Membrane Biology.* 26:121–151.

Koumi, S-i., R. Sato, Y. Kushikata, H. Muramatsu, T. Horikawa, T. Aramaki, and H. Okumura. 1990. The properties of voltage gated delayed rectifier outward current in guinea pig hepatocytes. *Biophysical Journal.* 57:315*a*. (Abstr.)

Koumi, S-i., R. Sato, T. Nagano, T. Horikawa, T. Aramaki, H. Okumura. 1991. Effective participation of Na^+/H^+ exchange on bile acid independent bile formation in guinea pig hepatocytes. *Biophysical Journal.* 59:93*a*. (Abstr.)

Marchetti, C., R. T. Premont, and A. M. Brown. 1988. A whole-cell and single-channel study of the voltage-dependent outward potassium current in avian hepatocytes. *Journal of General Physiology.* 91:255–274.

Mauger, J. P., F. Poggioli, F. Guesdon, and M. Claret. 1984. Noradrenaline, vasopressin and angiotensin increase Ca^{2+} influx by opening a common pool of Ca^{2+} channels in isolated rat liver cells. *Biochemical Journal.* 221:121–127.

McDonald, T. F., and W. Trautwein. 1978. The potassium current underlying delayed rectification in cat ventricular muscle. *Journal of Physiology.* 274:217–246.

Moore, R. D. 1983. Effects of insulin upon ion transport. *Biochimica et Biophysica Acta.* 737:1–39.

Noble, D., and R. W. Tsien. 1969. Outward membrane currents activated in the plateau range of potentials in cardiac Purkinje fibers. *Journal of Physiology.* 200:205–231.

Ogden, D. C., T. Capiod, J. W. Walker, and D. R. Trentham. 1990. Kinetics of the conductance evoked by noradrenaline, inositol triphosphate or Ca^{2+} in guinea-pig isolated hepatocytes. *Journal of Physiology.* 422:585–602.

Okabe, K., K. Kitamura, and H. Kuriyama. 1987. Features of 4-aminopyridine sensitive outward current observed in single smooth muscle cells from the rabbit pulmonary artery. *Pflügers Archiv.* 409:561–568.

Orrenius, S., P. Nicotera, and G. Bellomo. 1987. Regulation of intracellular Ca^{2+} homeostasis in hepatocytes and toxicological consequences of its perturbation. *In* Modulation of Liver Cell Expression. W. Reutter, H. Popper, I. M. Arias, P. C. Heinrich, D. Keppler, and L. Landmann, editors. MTP Press Limited, Lancaster, UK. 157–164.

Sandford, C. A., J. H. Sweiry, and D. H. Jenkinson. 1992. Properties of a cell volume-sensitive potassium conductance in isolated guinea-pig and rat hepatocytes. *Journal of Physiology.* 447:133–148.

Tohse, N. 1990. Calcium-sensitive delayed rectifier potassium current in guinea pig ventricular cells. *American Journal of Physiology.* 258:H1200–H1207.

Tsien, R. W., W. Giles, and P. Greengard. 1972. Cyclic AMP mediates the effect of adrenaline on cardiac Purkinje fibers. *Nature.* 240:181–183.

Ulbricht, W., and H-H. Wagner. 1976. Block of potassium channels of the nodal membrane by 4-aminopyridine and its partial removal on depolarization. *Pflügers Archiv.* 367:77–87.

Van Driessche, W., and W. Zeiske. 1985. Ionic channels in epithelial cell membranes. *Physiological Reviews.* 65:833–903.

Walsh, K. B., T. B. Begenisich, and R. S. Kass. 1988. β-Adrenergic modulation in the heart: independent regulation of K and Ca channels. *Pflügers Archiv.* 411:232–234.

Walsh, K. B., T. B. Begenisich, and R. S. Kass. 1989. β-Adrenergic modulation of cardiac ion channels: differential temperature sensitivity of potassium and calcium current. *Journal of General Physiology.* 93:841–854.

Weiss, S. J., and J. W. Putney. 1978. Does calcium mediate the increase in potassium permeability due to phenylephrine or angiotensin II? *Journal of Pharmacology and Experimental Therapeutics.* 207:669–676.

Yeh, J. Z., G. S. Oxford, C. H. Wu, and T. Narahashi. 1976. Dynamics of aminopyridine block of potassium channels in squid axon membrane. *Journal of General Physiology.* 68:519–535.

Young, S. H., and J. W. Moore. 1981. Potassium ion currents in the crayfish giant axon; dynamic characteristics. *Biophysical Journal.* 36:723–733.